

C. C. HANKE AND H. BICHSEL

PRECISION ENERGY LOSS
MEASUREMENTS FOR NATURAL
ALPHA PARTICLES IN ARGON

Det Kongelige Danske Videnskabernes Selskab
Matematisk-fysiske Meddelelser 38, 3



Kommissionær: Munksgaard
København 1970

TABLE OF CONTENTS

	Page
1. Introduction	3
2. Energy Loss Measurements	3
2A. Measurements of Energies	4
a) Determination of Energy $\langle T \rangle$ of Incident Alpha Particle	4
b) Determination of Residual Energies $\langle T_1 \rangle$	5
2B. Absorber Measurements	8
a) Apparatus	8
b) Gas Density	8
3. Corrections to the Experiment	10
3A. Multiple Scattering Correction	10
3B. Lewis Correction	10
3C. Corrected Experimental Results	12
4. Theoretical Interpretation	12
4A. Bethe Stopping Power Theory	12
4B. Particle Charge Dependence	13
4C. Charge Exchange Correction	13
4D. Fitting Procedure	14
5. Results	15
6. Discussion	18
6A. Range Measurements	18
6B. Stopping Power Measurements	19
6C. Hydrogen Ion Stopping Powers	19
6D. Theory	22
7. Conclusion	23
8. Acknowledgement	23
Appendix: Correction to the Pathlength due to Multiple Scattering	24
References	28

Synopsis

Energy losses of natural alpha particles from Bi^{212} and Po^{212} have been determined in argon gas with an accuracy of about 0.2%. The Lewis correction and the multiple scattering correction are briefly discussed. The data are compared with the Bethe theory, formulated with two different shell correction functions. I -values of 182 eV and 167 eV are obtained, respectively. Northcliffe's measurements at higher energies favor $I = 182$ eV. Comparison with hydrogen ion stopping power data confirms the recently discovered dependence on the particle charge.

1. Introduction

While the Bethe theory of stopping power^{1,2,3} is generally accepted, there are many details at low particle velocities which are not well established. In particular it is not clear how valid the Born approximation is. Accurate experiments are a necessity for the clarification of these questions. Furthermore, accurate measurements are needed for applications in nuclear physics, health physics, radiobiology, industrial radiation uses and related fields.

Energy loss and range measurements for natural alpha particles in many materials have been performed for over half a century^{4,5,6,7,8}. The development of solid state ionization detectors has permitted a more accurate measurement of particle energies and allows fairly simple experiments^{9,10,11,12}.

Data for precision measurements in gases are scarce^{13,14}. Consideration of the details in the detector operation permit an accuracy of close to 0.1% in the energy loss measurements (section 2).

With the parameters obtained in this work we present a range energy table for α -particles. Recently^{15,16} it has been confirmed, that stopping powers and ranges of particles with different charges z are not exactly proportional to z^2 , as the Bethe-formula predicts. A comparison with available proton and triton measurements will be shown.

2. Energy Loss Measurements

Bethe's theory furnishes the mean energy loss of initially monoenergetic particles in absorbers of a given thickness, and therefore will be applicable to the present experiment. While it is possible to determine energy losses directly, if the absorber can be used as a detector (ref. 17; an interesting variation is described by ANDERSEN, *et al.*¹⁸), in most substances it will be necessary to measure an incident energy T and a residual energy T_1 with mean values $\langle T \rangle$ and $\langle T_1 \rangle$ respectively. The mean energy loss will be determined by

$$\bar{A} = \langle T \rangle - \langle T_1 \rangle.$$

In the measurements presented here, absorber thicknesses will be expressed in mass per unit area. For gases, the distance d between the particle source and the surface of a silicon detector will have to be measured as well as the pressure of the gas.

2A. Measurements of Energies

The radioactive decay of Th C and Th C' nuclei is used as a source of alpha particles of well-known energies for the experiment. For the preparation of a source, a stainless steel pin with a diameter of 2 mm and a flat and polished end surface was connected to the negative pole of a 300 volt battery, and was exposed in the thorium emanation (Rn²²⁰) of a 10 mc Th²²⁸ source for 60 minutes.

a) *Determination of Energy $\langle T \rangle$ of Incident Alpha Particle.*

Since the thoron atoms attached to the source undergo two shortlived alpha decays (to Po²¹⁶ and Pb²¹², which has a half life for beta decay of 11 hours), it is to be expected that recoil nuclei will penetrate a small distance into the source. The alpha particles from Bi²¹² (Th C) and Po²¹² (Th C') used in the experiment therefore will often come from inside the stainless steel source pin. No direct evidence is available for Th sources, but Rytz¹⁹ found for Bi²¹¹ sources a mean energy which was about 3 keV lower than the energy of the "line head" (estimated by us from Fig. 7 of ref. 19). It will therefore be assumed that the energies given by Rytz have to be reduced by 3 keV and 4 keV for Po²¹² and Bi²¹², respectively. The values adopted for this paper are listed in Table I.

Measurements of the shape and the pulseheight of the Po²¹² line in the silicon detector showed no change as a function of the time used to prepare the source. The exposure of the source to argon gas for 12 hours also did not change the mean pulseheight.

TABLE I

Nucleus	T (keV) Rytz	Self Absorption	T (keV) Adopted	Relative Abundance
Po ²¹²	8785.4 ± 0.8	3 ± 2 keV	8782 ± 2	100 %
Bi ²¹² ₁	6089.8 ± 0.7	4 ± 3 keV	6086 ± 3	27.1 %
„ ₀	6050.6 ± 0.7	4 ± 3 keV	6047 ± 3	69.7 %

The separation of 39 keV for the two energies found for Bi^{212} can only be observed for zero energy loss. For finite energy losses, straggling amounts to considerably more than 39 keV, and it is necessary to use a weighted mean energy for the two energies. Using the branching ratio given by PERLMAN and ASARO²⁰ (see Table I), a mean energy $T = 6058$ keV, corrected for source thickness, is obtained.

b) *Determination of Residual Energies T_1 .*

The reduced energies T_1 are determined in a detection system consisting of a surface barrier silicon detector, test pulser, preamplifier, amplifier and a 100 channel analyzer. Since it was found that amplification changes of the system amounted to more than 1% per day, all measurements were based on a comparison of alpha pulseheights to test pulseheights. The quantity observed in the silicon detector is a charge pulse caused by the collection of the electrons and holes produced by the particle. The detailed detector performance will be discussed in connection with the energy calibration of the detector system.

Testpulses with a rise time comparable to the rise time of alpha-pulses (less than 0.1μ sec) are fed into the preamplifier in parallel with the alphas through a 1 pF capacitor. It has been assumed that testpulses and alpha-pulses of the same magnitude will experience exactly the same amplification in the system. No complete check of this assumption has been performed, but some tests on the same system are described by TSCHALÄR²¹. Problems within the accuracy desired here ($\sim 0.1\%$) occur for pulse rise times exceeding 0.1μ sec.

It is not practical to superimpose a testpulse group on the alpha group. Therefore, in each measurement, the group of alphapulses is bracketed by two groups of testpulses. Since the analyzing system is somewhat nonlinear, a third group of testpulses is also recorded. The testpulses are recorded during the period of the alpha measurement (Fig. 1). The magnitude of the testpulses is proportional to the dial setting of a helipot. Its linearity has been measured with a Wheatstone bridge and is better than 0.05%. The voltage for the testpulses is supplied from a Zener reference diode, its random drifts were slow during a day and amounted to less than 0.05%.

The following evaluation procedure is used for the determination of the mean alpha-pulseheight for each spectrum.

- i) Calculate the mean channel number for the alphas and the three testpulse groups.

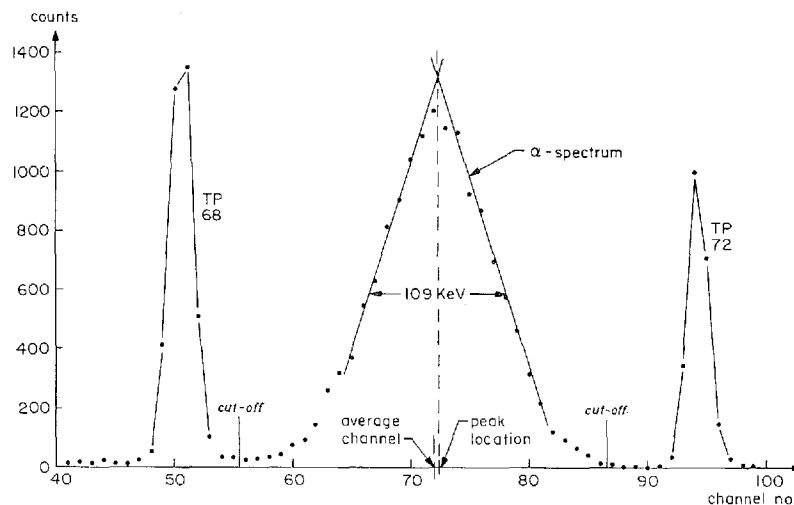


Fig. 1. Typical spectrum of alpha particles reduced in energy from $\langle T \rangle = 8.782$ MeV to $\langle T_1 \rangle \sim 7.0$ MeV. Thus, the average energy loss is about 1.8 MeV. With the indicated cut-off points for the spectrum, the location of the mean channel is calculated to be 72.01. The "peak location" obtained by visually drawing tangent lines to the sides of the spectrum is located at 72.3 channels. The full width at half maximum obtained from the figure is 109 keV, while the calculated standard deviation for the spectrum is $\sigma = 48.4$ keV. The ratio of these two numbers is 2.26. For a gaussian, this ratio is 2.36. Two testpulses with dial readings of 68 and 72 are also shown.

- ii) Calculate a quadratic calibration curve for the conversion of channel number into dial setting of testpulses.
- iii) Express mean alpha channel number as the dial setting of a testpulse that would give the same mean channel number.

For all the spectra recorded in a particular run (typically about 30 spectra, measured during 8 hours), an absolute energy calibration was obtained in the following manner.

The stopping of the α -particles in the detector material is mainly due to inelastic collisions with silicon electrons, which result in the charge pulse collected at the detector surfaces. LINDHARD *et al.*²² calculated the energy loss due to nuclear collisions which can not be detected by this method. The theoretical values have been confirmed at lower energies²³. In our energy range this "ionization defect" is 9–13 keV, increasing with energy. The incident energies of table I have to be reduced respectively, because we must find the linear relationship between the α -pulseheights on the multichannel analyzer and the electronic energy loss in the detector.

The calibration energies were also corrected for the undetected energy losses in the gold surface layer and the adjoining deadlayer in the detector

material²⁴. They were determined experimentally by observing the line shift of alphas incident at different angles. The total thickness corresponds to about $100 \mu\text{gcm}^{-2}$ gold, and gold stopping power²⁵ was used to find the energy loss for other alpha energies.

A linear least squares fit was calculated for the pulseheights (expressed in equivalent dial readings) versus the corrected calibration energies. An energy calibration factor f is thus obtained. Zero energy was assigned to a testpulse dial setting of zero.

Occasionally, during a day's observation, a drift of the energy calibration factor amounting to a few kilovolts at 9 MeV could be seen. This was corrected for by interpolating the energy calibration with respect to the time of the day, so that every run effectively had its own calibration. If the drift amounted to more than 10 keV, the measurements would be rejected. The average standard deviation of the energy calibration runs is between 2 and 5 keV. Second order fits did not improve the standard deviations.

On one occasion, calibrations with a commercial Th^{228} source were performed, using the α -lines at 5.338 MeV and 5.421 MeV (Ref. 20). Their pulseheights agreed with the usual calibration within 2 keV.

For the alpha particles travelling through the gas, the mean energy $\langle T_1 \rangle$ is calculated from the equivalent dial reading of the mean alpha pulseheight, adding the calculated energy loss in the detector surface layer and deadlayer, and the ionization defect.

In addition to the uncertainty due to the energy calibration, a systematic error is introduced due to the choice of cutoffs of the distribution functions $f(T_1)$ of the reduced energies T_1 at finite values T' and T'' . $f(T') = f(T'')$ are usually between 5% and 10% of the peak value of $f(T_1)$; thus $\langle T_1 \rangle$ is determined by

$$\int_{T'}^{T''} f(T_1) T_1 dT_1 / \int_{T'}^{T''} f(T_1) dT_1.$$

CUETHAM-STRODE *et al.*²⁶ investigated low energy tails of various α -spectra from silicon detectors, and found, that the mean energy of a 6 MeV α -source decreased 0.07% relative to the mean energy derived from the symmetric part of the spectrum. If we assume the same relative decrease for all energies, this correction is negligible, when we do not take the tails into account in the energy calibration.

The most probable energy $T_{1,\text{mode}}$ for the energy spectra was determined by the limit of the mean energy, when the distance between the cut-off energies T' and T'' was narrowed, so that the values of the distribution functions at these energies, $f(T') = f(T'')$, increased from 10% to 100% of

the peakvalues. We compared $T_{1, \text{mode}} - \langle T_1 \rangle$ with TSCHALÄR's²⁷ calculations, based on the classical collision spectrum with free absorber electrons. The deviations were less than 2 keV for higher $\langle T_1 \rangle$, increasing to 5 keV for the lowest $\langle T_1 \rangle$. They are probably caused by the neglect of the resonance contribution to the straggling in TSCHALÄR's theory.⁶⁵

Uncertainties caused by the statistical nature of the number of counts in each channel are estimated to be less than 1 keV.

2B. Absorber Measurements

a) *Apparatus.*

A stainless steel vacuum chamber about 9 cm in diameter and 32 cm in length was used for the measurements. The silicon detector is mounted on one of the end plates. The source is installed in a holder attached to a lead screw with a pitch of approximately 1 mm. The lead screw was connected to a counter, indicating tenths of revolutions. The screw was calibrated every measuring day using a stainless steel tube as a gauge block between the source holder and the detector mount. The length of the gauge tube was measured with a micrometer screw within 0.03 mm.

The distance from the detector mount to the gold layer of the detector surface was measured with a microscope, whose focus system was attached to a dial indicator. The distance was found, by focussing on the detector mount and on the gold layer, respectively, to be $1.54 \pm .02$ mm.

Distances d between 8 and 25 cm were used. No discrepancies connected with d were observed within the experimental accuracy. The over-all accuracy is estimated to be 0.04 mm. Since the detector used had a diameter of about 5 mm, the distance from source to detector varies slightly over the detector surface. The maximum correction in d would amount to 0.05% for the edge of the detector surface. No correction for this effect has been made.

b) *Gas Density.*

Commercial compressed argon gas with a stated purity of 99.995% was used for the measurements. Impurities should falsify the data by less than 0.01%. The vacuum system was evacuated to better than $5 \cdot 10^{-5}$ atm before filling with argon. Also, it was flushed three times before the final filling was introduced. Leakage of the system, including outgassing, amounted to less than $5 \cdot 10^{-6}$ atm per hour.

The argon gas pressure p was measured with a mercury manometer, which consisted of two vertical glass tubes (inside diameter about 1.87 ± 0.02 cm) filled with doubly distilled mercury. The height of each mercury

column was measured by observing through a cathetometer telescope, simultaneously, the top of the meniscus and a stainless steel meterstick mounted next to the glass tubes. The accuracy of the measurement is about ± 0.01 cm. Capillary corrections are estimated to be less than 0.003 cm, and the density of mercury was temperature corrected.

The temperature t of the gas was measured with a mercury-in-glass thermometer to within 0.1°C . Thermocouples were used to monitor the temperature at different places on the vacuum system. No gradients greater than 0.1°C were observed. For the calculation of the gas density ρ , the Van der Waals equation is used in the following approximate form:

$$\rho = \rho_0(1 + \rho_0^2 a/pA^3) (1 - b\rho_0/A) \quad (1)$$

where A = atomic weight of argon = 39.948 g/mole, $\rho_0 = Ap/RT$, p = gas pressure in atm, $R = 0.08206$ l atm/mole $^\circ\text{K}$, T = gas temperature in absolute scale, a = first Van der Waals coeff. = 1.345 l² atm/mole², and b = second Van der Waals coeff. = 0.03219 l/mole. The difference between the liter l and the cubic decimeter dm³ has been neglected. Since at 1 atm, the Van der Waals correction amounts to only 0.123%, the first approximation to the density given by eq. (1) is sufficient.

The final absorber thickness s is derived by the product of the corrected distance d and the density ρ : $s = d \cdot \rho$.

The experimental errors of the measured energies and absorber thicknesses are summarized in Table II.

TABLE II
Errors Associated with Energy Loss Measurements.

	Errors	
	Absolute	Relative
Pressure Measurement		
Height of Columns	± 0.1 mm	0.01 to 0.1%
Density of Mercury	± 0.002 cm ⁻³	0.01%
Temperature Measurement	$\pm 0.1^\circ\text{K}$	0.03%
Distance Measurement	± 0.04 mm	0.02 to 0.04%
Energy Measurement		
5 MeV $< T_1 < 9$ MeV	± 2 keV	0.04%
1 MeV $< T_1 < 5$ MeV	± 5 keV	0.1 to 0.5%

3. Corrections to the Experiment

Since the Bethe theory provides the integrated energy loss along the path of particles, corrections have to be estimated for the experimental data: for multiple scattering and for discrete energy loss (Lewis correction).

3A. Multiple Scattering Correction

During their passage through the gas, the particles experience many small changes in the direction of their velocity, caused by Coulomb scattering by the nuclei. This results in pathlengths longer than the thickness of material traversed. The α -particles are not all emitted in the direction of the detector, and the multiple scattering distribution functions have to be integrated over the incident angles as well as the exit angles. This case has been treated by ØVERÅS²⁸, not taking energy loss into account. The method has been extended including the energy loss, as shown in the Appendix. The difference between mean pathlength and perpendicular absorber thickness s amounts to $8 \mu\text{gcm}^{-2}$ for $\langle T \rangle = 8.78 \text{ MeV}$ and $\langle T_1 \rangle = 1 \text{ MeV}$. The correction decreases rapidly for increasing $\langle T_1 \rangle$ and is negligible for $\langle T_1 \rangle \gtrsim 3 \text{ MeV}$.

3B. Lewis Correction

The Bethe theory provides the mean energy loss of particles in a thin absorber; for thick absorbers we have to integrate the inverse stopping power function, as if there was a continuous slowing down of the particles ("csda approximation"). The increasing energy spread of the initially monoenergetic particles will in a finite absorber cause a difference between the mean csda energy loss and the actual energy loss. LEWIS²⁹ has given a derivation of this effect, using the classical single collision law:

$$P(Q, T) = k/(2T \cdot Q^2)$$

where Q is the energy transferred to an electron and $k = 2\pi NZ z^2 e^4 M/m$ [see eq. (3)]. For *small* energy losses (less than 800 keV for our problem), T is approximately constant, and $P(Q, T)$ will be constant. Then the experimental spectrum $\varphi(Q, T)$ will give the same average energy loss as the csda calculation.

For *larger* energy losses the T -dependence of $P(Q, T)$ makes the distribution broader, and a tail appears at the low energy end of the spectrum. $\langle T_1 \rangle$ thus becomes lower than the theoretical csda energy, which is used for the further evaluation of the experimental data.

TABLE III

Corrected energy loss data for α -particles in Argon. $\langle T \rangle$ is the incident α -energy corrected for selfabsorbtion and $\langle T_1 \rangle$ is the average energy at the detector surface after passing through the gas. Corrections for the detector surface layer and the ionization defect are included in $\langle T_1 \rangle$. s is the gas thickness corrected for multiple scattering to give the mean pathlength. Two sets of measurements are presented.

$\langle T \rangle = 6.058 \text{ MeV}$		$\langle T \rangle = 8.782 \text{ MeV}$	
s mgcm^{-2}	$\langle T_1 \rangle$ MeV	s mgcm^{-2}	$\langle T_1 \rangle$ MeV
7.617	1.044	13.948	1.358
7.576	1.095	13.748	1.589
7.192	1.526	13.202	2.074
6.608	2.071	12.718	2.465
6.559	2.104	11.976	3.040
5.995	2.573	11.168	3.588
5.297	3.089	10.446	4.038
4.625	3.545	9.590	4.533
3.810	4.054	8.733	4.997
3.016	4.515	7.779	5.490
1.995	5.072	6.660	6.029
1.070	5.542	5.661	6.490
		4.442	7.028
		3.207	7.539
		1.973	8.041
		0.659	8.539
7.768	0.864	14.014	1.310
7.254	1.477	13.167	2.124
6.698	2.006	10.630	3.936
6.144	2.468	10.470	4.022
5.513	2.943	9.942	4.341
4.808	3.422	8.969	4.879
4.006	3.935	7.887	5.445
3.140	4.450	6.871	5.938
2.217	4.960	6.797	5.972
1.258	5.448	5.784	6.440
		4.696	6.920
		3.698	7.339
		2.348	7.888
		1.014	8.401

The positive correction to $\langle T_1 \rangle$ gives a negative correction to the energy loss and to the stopping power used for computation of the theoretical mean range

$$R = \int_0^{\langle T \rangle} [1/S(T')]dT'. \quad (2)$$

Therefore the integrand in (2) will increase due to the correction, and R will be slightly larger. This effect was discussed by LEWIS²⁹ for the total range of a charged particle. TSCHALÄR²⁷ calculated the correction to $\langle T_1 \rangle$ by a similar method. According to his results, the increase of $\langle T_1 \rangle$ is less than 0.5 keV for $\langle T_1 \rangle \sim 1$ MeV, and smaller at higher values. No correction therefore is applied for this effect.

3C. Corrected Experimental Results

An experimental data point consists of three numbers: a) initial alpha particle energy $\langle T \rangle$, b) corrected mean energy $\langle T_1 \rangle$ of alpha particles after the absorber, c) corrected mean pathlength s . A list of the data points is given in Table III. No empirical range energy relation is presented; instead a comparison with Bethe's theory will be presented in Section 5. No independent data are available for a direct comparison. A comparison with other data, using the theory, will be given in Section 6. The results deviate slightly from those reported in ref. 30 due to previous errors in the data treatment.

4. Theoretical Interpretation

4A. Bethe Stopping Power Theory

Bethe's theory is used for the interpretation of the data. The basic formulation for the stopping power $S = -dT/ds$ follows from the Born approximation:

$$S = 4\pi e^4(z^2/mv^2) \cdot N \cdot B \quad (2)$$

where e and m are electron charge and mass, z and v charge number and velocity of the particle, N the number of stopping atoms per cm^3 and B the stopping number. In the quantum mechanical theory (see e.g. ref. 2) B is defined as³¹

$$B = Z \ln(2mv^2/I) - \sum_i C_i \quad (3)$$

where Z is the atomic number of the absorber, I the average ionization potential, and C_i the so-called shell corrections, one term for each electronic shell of the absorber atom. For argon, the following expression is obtained:

$$S = (0.30706 z^2/A\beta^2) \cdot \{Z[f(\beta) - \ln 1] - C_K - C_L - C_M\} \quad (4)$$

where A is the atomic mass of argon, β is v relative to the velocity of light in vacuum, and $f(\beta) = \ln 2mc^2\beta^2/(1 - \beta^2) - \beta^2$.

For C_K and C_L , WALSKÉ's values^{32,33} can be used approximately. No reliable theoretical determination of I and C_M are available. Since KHANDELWAL's calculation³⁴ of C_M is based on hydrogenic wave functions, it cannot be considered to be applicable to argon. Even the L -shell correction is not strictly applicable, but it will be practical as a first approximation.

4B. Particle Charge Dependence

According to the Bethe formula (2) the stopping power is proportional to the square of the particle charge z , since B as defined in (3) only depends on the particle velocity. Recently HECKMAN and LINDSTROM¹⁵ discovered differences in the stopping powers of positive and negative pions at the same velocity, and ANDERSEN *et al.*¹⁶ also detected deviations from the theoretical charge dependence for hydrogen and helium ions. The latter authors indicate, that the discrepancy is present in previous data, although the errors are of the same order of magnitude as the deviations.

This effect is not taken into account in the present data treatment, since no satisfactory theoretical approach is available. The following presentation of stopping powers and ranges is thus strictly confined to α -particles. In section 6 a comparison with available hydrogen ion data will be presented.

4C. Charge Exchange Correction

When the α -particles slow down below 2 MeV, they begin to capture electrons from the gas atoms, and subsequently lose electrons also. By this process the α -particles suffer energy losses in addition to the normal electronic stopping, and Bethe's formula cannot be used, even if the average charge of the He-ions is known. However, it is practical to apply the total correction to z^2 in eq. (2), and WHALING's table³⁵ for determination of S for α -particles from proton stopping powers is used. WHALING's table is an average over a collection of experimental data, and the charge corrections are estimated to be within 20 % of the tabulated values. Intermediate values were determined from the table by linear interpolation.

4D. Fitting Procedure

For the comparison with the experimental data, two methods of approximation for shell corrections will be used. In both cases, I is a parameter to be determined from experiment, and WALSKE's C_K is assumed to be correct.

Method 1 It will be assumed that the shell corrections for the L and M -electrons can be combined into one function:

$$C_{L+M} = V_L \cdot C_L(H_L \cdot \beta^2) \quad (5)$$

where C_L is WALSKE's L -shell function and V_L and H_L are parameters determined from experiment.

Method 2 WALSKE's C_L is assumed to be correct and an M -shell correction is determined with two parameters V_M and H_M :

$$C_M = V_M \cdot C_L(H_M \cdot \beta^2) \quad (6)$$

where again H_M and V_M are determined from the experiment.

A Fortran program similar to the one described in ref. 36 was used for the evaluation of the experimental data and the comparison with theory. The theoretical range difference r , obtained by integrating over the stopping power S (eq. (2)), using the experimental energies $\langle T \rangle$ and $\langle T_1 \rangle$:

$$r = \int_{\langle T_1 \rangle}^{\langle T \rangle} S^{-1} dT \quad (7)$$

was compared with s , the experimental pathlength.

A least squares fit was obtained for the three parameters I , and H_L , V_L of eq. (5), or H_M , V_M of eq. (6), using $\chi^2 = \sum (r-s)^2$ to find the minimum. The weighting factor is approximately constant, and assumed to be 1. Furthermore the program computed the sum of the estimated shell-corrections, divided by Z , plotted in Fig. 6. Due to the large errors in the charge exchange corrections, the experimental measurements for $\langle T_1 \rangle \lesssim 2$ MeV should have a weighting factor less than 1, but this was omitted.

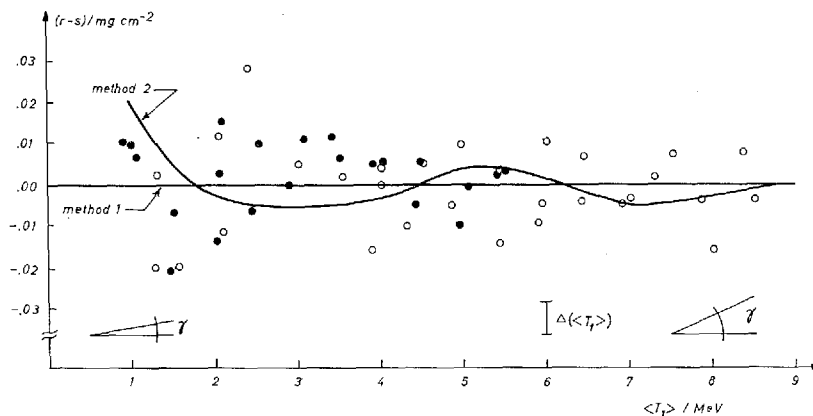


Fig. 2. Least squares fit of range difference measurements in argon. r is the calculated range difference [from eq. (7)]. The horizontal line at 0.00 mgcm^{-2} represents the fit, where the L and M -shell corrections are combined into one function, C_{L+M} (method 1). The other curve appears, when Walske's C_L is assumed to be correct, and the M -shell correction is fitted separately (method 2). Method 1 and method 2 have rms errors 8.7 and $9.1 \mu\text{gcm}^{-2}$, respectively. $\Delta(\langle T_1 \rangle)$ indicates the estimated error in $(r-s)$ due to the total error in the energy measurements. The slope zero of the horizontal line represents the inverse of the stopping power S in Table IV, and the tangent of the angle γ indicates an 0.3% change of S at the energies 1 and 9 MeV , respectively. ●: incident α -energy $\langle T \rangle = 6.058 \text{ MeV}$; ○: $\langle T \rangle = 8.782 \text{ MeV}$.

5. Results

The evaluation of the experimental data according to Method 1, using Walske's C_K and scaling C_L with two parameters to obtain a best fit, yields $I = 182 \text{ eV}$, $H_L = 1.6$, $V_L = 1.2$. The rms deviation is $\xi = \pm 8.7 \mu\text{gcm}^{-2}$. Values of $q = r - s$ are plotted versus residual mean energy $\langle T_1 \rangle$ in Fig. 2. r is computed according to eq. (7). Total ranges

$$r_t = \int_1^T S^{-1} dT + R(1 \text{ MeV}) \quad (8)$$

with $R(1 \text{ MeV}) = 0.85 \text{ mgcm}^{-2}$ and the stopping power S obtained in the course of the calculation are given in Table IV.

It can be shown mathematically³⁷, that experimental rms deviations ΔS of S are those in Table IV, and they agree with the estimated errors obtained empirically by drawing curves of different shapes through the experimental points of Fig. 2.

It is quite obvious from eq. (4), that small changes in I can be compensated for by corresponding changes in the shell corrections over a limited

TABLE IV

Stopping power and range as a function of energy for α -particles in argon. S are the theoretical values using eq. (11) (Method 1), and ΔS are the estimated rms deviations of S . The range is defined by eq. (8). The value 0.846 mgcm^{-2} for 1 MeV is adopted from a comparison with total mean ranges from ref. 38 (see section 6)

α -energy MeV	S keV/mgcm^{-2}	ΔS %	Range mgcm^{-2}
1.0	1169	...	0.846
1.25	1103	1.5	1.067
1.5	1039	0.8	1.299
2.0	901	0.3	1.820
2.5	793	"	2.413
3.0	715	"	3.078
3.5	654	"	3.810
4.0	605	"	4.606
4.5	564	"	5.462
5.0	529	"	6.379
5.5	498.7	"	7.353
6.0	472.2	"	8.384
6.5	448.9	"	9.470
7.0	428.0	"	10.62
7.5	409.3	"	11.81
7.75	402.6	"	12.47
8.0	392.3	0.8	13.06
8.5	369.7	...	15.03
8.75	376.9	1.5	14.36

energy range. Thus, e.g., for this method, a local minimum is also found at $I = 179$ eV, $H_L = 1.6$, and $V_L = 1.3$ with $\xi = \pm 8.8 \mu\text{gcm}^{-2}$. Therefore it is not possible to assign unambiguous errors to the experimentally determined parameters.

The second method (using Walske's C_K and C_L , and C_M scaled from C_L) yields an I -value of 167 eV with $H_M = 3.6$ and $V_M = 1.1$. The rms deviation ξ is $\pm 9.1 \mu\text{gcm}^{-2}$.

The analysis of MARTIN and NORTHCLIFFE's α -particle data³⁹ using Walske's unmodified C_K and C_L gave an I -value of 184 eV⁴⁰. This indicates that Method 2 overestimates the shell corrections, and the not unexpected conclusion is that C_L cannot be used for $Z = 18$ without modification.

TABLE V

Stopping power S in $\text{keV}/\text{mgcm}^{-2}$ and ranges in mgcm^{-2} for α -particles in argon computed using the program of ref. 36 with $I = 182$ eV, Walske's K-shell correction and the L-shell correction fitted to the present experimental data.

Energy MeV	S	Range	Energy MeV	S	Range	Energy MeV	S	Range
1.0	1169	0.85	10	337.8	18.57	100	60.3	937.6
1.1	1137	0.93	11	316.4	21.63	110	60.0	1110
1.2	1111	1.02	12	297.9	24.89	120	52.3	1295
1.3	1092	1.11	13	281.7	28.34	130	49.11	1492
1.4	1074	1.21	14	267.3	31.99	140	46.35	1702
1.5	1039	1.30	15	254.5	35.82	150	43.92	1924
1.6	1005	1.40	16	243.0	39.84	160	41.77	2157
1.7	974	1.50	17	232.6	44.05	170	39.84	2403
1.8	944	1.60	18	223.1	48.44	180	38.11	2659
1.9	922	1.71	19	214.5	53.01	190	36.55	2927
2.0	901	1.82	20	206.6	57.77	200	35.13	3206
2.2	854	2.05	22	192.6	67.80			
2.4	811	2.29	24	180.6	78.53			
2.6	776	2.54	26	170.1	89.95			
2.8	744	2.80	28	160.9	102.0			
3.0	715	3.08	30	152.8	114.8			
3.2	689	3.36	32	145.5	128.2			
3.4	665	3.66	34	139.0	142.3			
3.6	643	3.96	36	133.1	157.0			
3.8	623	4.28	38	127.7	172.3			
4.0	605	4.61	40	122.8	188.3			
4.2	588	4.94	42	118.3	204.9			
4.4	571	5.29	44	114.1	222.1			
4.6	556	5.64	46	110.3	240.0			
4.8	542	6.01	48	106.8	258.4			
5.0	529	6.38	50	103.4	277.4			
5.5	498.7	7.35	55	96.1	327.6			
6.0	472.2	8.38	60	89.8	381.5			
6.5	448.8	9.47	65	84.4	438.9			
7.0	428.0	10.61	70	79.7	499.9			
7.5	409.3	11.81	75	75.5	564.4			
8.0	392.3	13.06	80	71.8	632.3			
8.5	376.9	14.36	85	68.5	703.7			
9.0	362.7	15.71	90	65.5	778.3			
9.5	349.8	17.11	95	62.8	856.3			

Thus for argon, the three parameters to be used for a calculation of stopping power for α -particles are

$$\begin{aligned} I &= 182 \text{ eV} \\ H_L &= 1.6 \\ V_L &= 1.2 \end{aligned}$$

Table V gives the stopping powers and ranges for 0.5–200 MeV α -particles computed with the above values for the parameters according to Method 1. In ref. 30 tables for hydrogen ions are calculated with the same parameters, not taking into account the charge dependence of the particles.

6. Discussion

6A. Range Measurements

Experimental measurements of extrapolated ranges by HARPER and SALAMAN⁴ for Po²¹⁰, Bi²¹² and Po²¹² alphas in argon were modified to yield mean ranges by BOGAARDT and KOUDJIS³⁸. Since the present data are range difference measurements, the range for 1 MeV alphas was estimated by adjusting Bogaardt's values to our data. This value is 0.846 mgcm⁻², and the resulting range energy curve agrees within 0.03 mgcm⁻² with Bogaardt's ranges. The error estimated by Bogaardt is 0.07 mgcm⁻². An earlier evaluation of Bogaardt's data using Walske's C_K and C_L gave a value $I = 183 \text{ eV}$ ⁴⁰. Fig. 3 presents a comparison with other range data R on this basis. Our results r_i correspond to the horizontal line at 0.00 mgcm⁻² framed by dotted lines at a distance of $r_{ms} = 0.009 \text{ mgcm}^{-2}$.

MANO⁴¹ measured range differences for several α -sources, and BOGAARDT³⁸ fitted the results to HARPER and SALAMAN's mean ranges. The good agreement with our range-energy relation at 10.538 MeV indicates, that the errors of the stopping powers at the upper limit of our energy range is considerably lower than estimated in table IV.

Several extrapolated range measurements for Po²¹⁰ ^{42, 43, 44, 45} reduced to mean ranges fluctuate with errors around 0.05–0.10 mgcm⁻², giving an error of the same order of magnitude to the above determined, initial 1 MeV-range. The α -energy value was taken from RYTZ¹⁹ and corrected for selfabsorption as described in section 2A. a).

BERTOLINI and BETTONI⁴⁶ measured ranges up to 3.5 MeV within 3%, in reasonable agreement with our results.

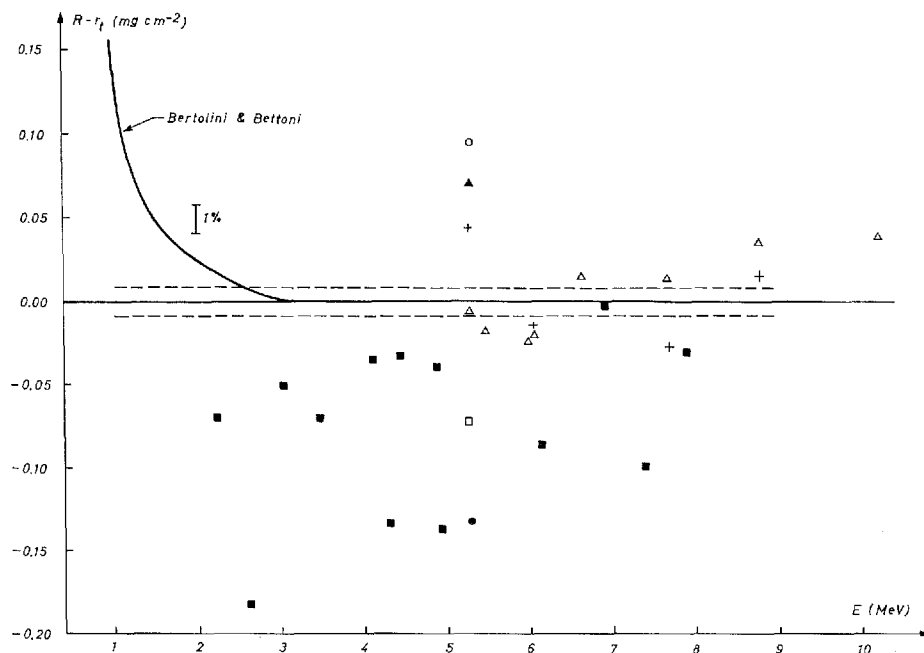


Fig. 3. Range measurements for α -particles in argon. Other data R are compared with present results r_t from Table V. $R - r_t$ is plotted versus the α -energy E . The dotted lines indicate the $rms = 0.009 \text{ mgcm}^{-2}$ of the present results. +: HARPER and SALAMAN⁴; Δ : MANO⁴¹; \circ : NAIDU⁴²; \square : COLBY and HATFIELD⁴³; \bullet : SCHMIEDER⁴⁴; \blacktriangle : EICHHOLZ and HARRICK⁴⁵; \blacksquare : CHANG¹⁴. The fully drawn curve below 3.5 MeV represent the ranges measured by BERTOLINI and BETTONI⁴⁶.

CHANG¹⁴ measured range differences s_{ch} with the same α -source energies and the results can be plotted in Fig. 3 directly, without introducing any initial alpha range. The deviations are so large, that some of the points could not be plotted on the scale. The fractional difference $(r - s_{ch})/r$ (eq.(7)) is approximately constant ($1 - 2\%$), indicating a systematic error due to the measurements of R .

6B. Stopping Power Measurements

Figure 4 shows available stopping power data in our energy range. Curve 1 are the results of BERTOLINI and BETTONI⁴⁶; from the error of their range measurements an overall error of about 5% can be estimated³⁷ for the stopping powers. They are in reasonable agreement with curve 2, a plot of table V, where the dotted curves indicate the estimated standard deviations. Curve 3 are values from RAMIREZ *et al.*⁴⁷; no errors are reported.

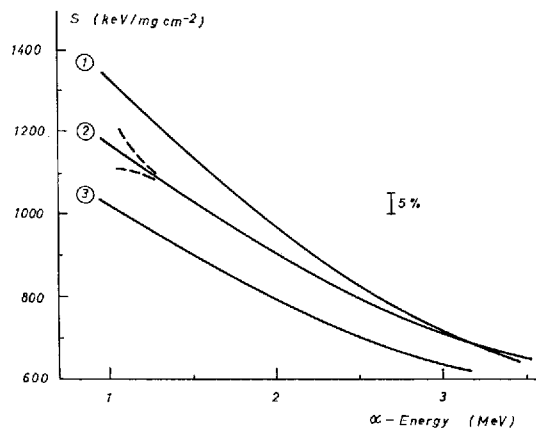


Fig. 4. Experimental stopping powers S of α -particles in argon versus α -energy. Curve 1: BERTOLINI and BETTONI⁴⁶, curve 2: present results (errors indicated with dotted curves), and 3: RAMIREZ *et al.*⁴⁷.

6C. Hydrogen Ion Stopping Powers

Recently^{15,16} it has been confirmed, that stopping powers of ions with different charges but the same velocity do not exactly follow the simple charge dependence of the Bethe formula (2). For a comparison we make use of the following procedure adopted from ref. 16.

We define the quantity L as

$$L = B/Z = f(\beta) - \ln I - C/Z$$

where B is the stopping number in eq. (3), and $C = \sum_i C_i$, the sum of the shell-corrections. L can be determined from eq. (2), when the experimental stopping power S is known. ANDERSEN *et al.*¹⁶ have shown, that the difference between L for helium ions L_{He} and L for hydrogen ions L_H at the same particle velocity is almost independent of the absorber material. A plot of L -differences is shown in Fig. 5. Curve 1 is an average over Andersen's aluminium and tantalum measurements, and the open circles indicate the data of ref. 15 giving the L -difference for negative and positive pions, $L_{\pi^-} - L_{\pi^+}$, in nuclear emulsion. If we assume, that the particle charge correction is a linear function of z , we can from Andersen's and Heckman's measurements estimate $L_o - L_H$, the correction of L for some artificial particles with zero charge.

Several hydrogen ion stopping power data for argon were compared with the present results by derivation of $L_{He} - L_H$. WOLKE *et al.*⁴⁸ measured triton

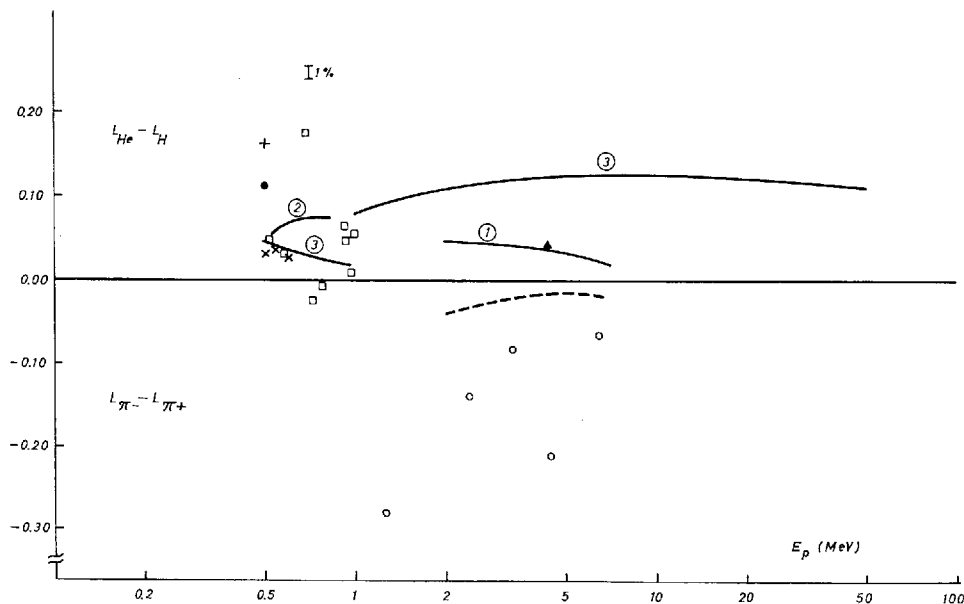


Fig. 5. Comparison of stopping powers in various materials for particles with different charges and identical velocities. The difference $L_{He} - L_H$ and $L_{\pi^-} - L_{\pi^+}$ as defined in section 6 is plotted versus equivalent proton energy $E_p = (M_p/M) \cdot E$ (M and E mass and charge of appropriate ion). Curve 1: ANDERSEN *et al.*¹⁶; curve 2: WOLKE *et al.*⁴⁸/present; curve 3: JANNI⁵³/present; - - - $1/Z (C^{(He)} - C^{(B)})$ as defined in section 6D; ○: HECKMAN and LINDSTROM²⁵; +: Cu and ●: Au from EHRHARDT *et al.*²⁵/GREEN *et al.*⁵²; ×: REYNOLDS *et al.*⁴⁹/present; □: CHILTON *et al.*⁵⁰/present; ▲: BROLLEY and RIBE⁵¹/present. The errorbar indicates the effect of a 1% change in the stopping power of one particle.

ranges* and evaluated the stopping powers in the range 0.5–0.8 MeV equivalent proton energies. Stopping powers of protons are reported by REYNOLDS *et al.*⁴⁹ at 0.5–0.6 MeV, by CHILTON *et al.*⁵⁰ at 0.5–1 MeV, and by BROLLEY and RIBE⁵¹ at 4.43 MeV. Brolley and Ribe's data have to be compared with the α -stopping power value of table V at 17.7 MeV, i.e. outside our experimental energy range.

For all argon data the errors of the proton measurements are of the same order of magnitude as the difference $L_{He} - L_H$, but from figure 5 is seen, that the effect is systematic and significant. At $E_p = 0.5$ MeV we have included the differences for some α -particle and proton measurements in Cu and Au^{52, 25}, indicating the weak dependence of the stopping material.

JANNI's table of proton stopping powers in argon⁵³ is also compared with the present measurements (curve 3 of fig. 5). They are semiempirical results from scaling and interpolating the shell-corrections for $E_p \gtrsim 1$ MeV. At $E_p =$

* Tabulated data received by private communication.

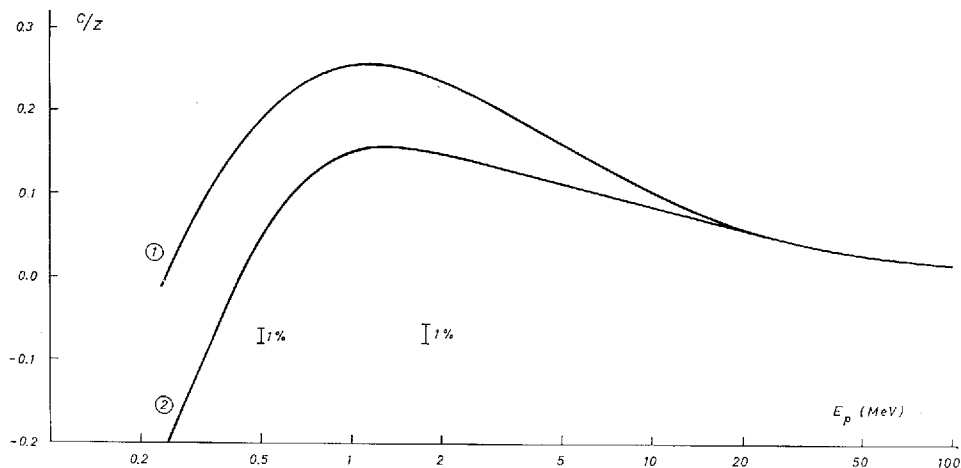


Fig. 6. Sum of shell-corrections C to the stopping power formula (5), divided by Z , versus reduced energy $E_p = (M_p/M)E$, as defined in figure 5. Curve 1: BONDERUP⁶⁷; curve 2: present, derived from the fitting procedure described in section 4D.

1 MeV a discontinuity appears, because the scaling method could not be applied in this region.

Recently SWINT *et. al.*⁶⁶ measured proton stopping powers for argon in the energy range 0.6–3.4 MeV. Their data are several percent higher than the measurements by other authors, and this would give L -differences far below zero on fig. 5.

6D. Theory

Although no theoretical treatment of the particle charge dependence is available, a selection of theoretical computations of I -values and shell-corrections is presented.

DALTON and TURNER⁵⁴ reanalyzed a series of high and medium-energy proton data for argon, and made use of FANO's³ asymptotic shell corrections for the entire atom. Their I -value for argon is 189 eV, but no measurements were used for the computation, where the protons were in the same velocity range as our α -particles.

A theoretical calculation of I has been done by BELL⁵⁵, using a procedure suggested by DALGARNO⁵⁶ for interpolation of I from known oscillator strength sums in Bethe's theory. Bell reports $I = 196 \pm 23$ eV.

BONDERUP⁵⁷ performed calculations of electronic stopping powers for heavy charged particles to quite low energies, by refining the procedure suggested by LINDHARD and SCHARFF⁵⁸, which makes extensive use of statis-

tical models of the atom. He presented his results as the shell corrections $C^{(B)}$ to the original Bethe formula, and used the I -value as a parameter*. They are plotted in Figure 6 versus equivalent proton energy E_p together with the present shell corrections from the fitting procedure described in section 4 D, divided by Z . Since Bonderup's shell corrections are the same for different charged particles at the same velocity, it might be valuable to assign the calculations to particles with zero charge correction.

ANDERSEN *et al.*¹⁶ indicated, that stopping powers for low charged particles were identical at the same velocities for $E_p \gtrsim 50$ MeV, and we conclude, that the L -differences in Figure 5 are negligible for high energies. Also the shell-corrections are smaller than the experimental errors for high E_p (ref. 3), and according to the definition of L -differences it is then reasonable to assign identical I -values for different charged particles. The L -differences, e.g. $L_{He} - L_H$, are thus actually the differences in the shell-corrections ($C^{(H)} - C^{(He)}$), divided by Z . By this interpretation we have in Figure 5 plotted the difference $(1/Z) \cdot (C^{(He)} - C^{(H)})$ (dotted) with curve 1 as zero line; it is seen, that the resulting curve coincides with that zero charge correction, one could obtain from interpolation of Andersen's and Heckman's L -differences - in agreement with the assignment of BONDERUP's shell corrections $C^{(B)}$ to zero charged particles.

7. Conclusion

Energy losses up to 7.5 MeV of 6.058 MeV and 8.782 MeV α -particles in argon have been measured within 2-5 keV. After correction of the data for multiple scattering, a fitting procedure using the Bethe theory for stopping powers gave the mean excitation potential $I = 182$ eV, and the shell-corrections. The derived stopping powers are within 0.3% for 2-8 MeV α -particles. The comparison with other proton stopping power data is in agreement with the newly confirmed differences in stopping powers of different charged particles with identical velocities.

8. Acknowledgement

C. C. H. wants to thank dr. H. H. ANDERSEN for our valuable discussions and private communications.

* BONDERUP kindly sent us his computation of the shell-corrections.

APPENDIX

Correction to the Pathlength due to Multiple Scattering

Several authors have treated multiple scattering corrections to the pathlength of a beam of charged particles incident at right angles to a plane-parallel slab of material^{59, 60, 61, 62}. In our case, however, it is a reasonable approximation, that the α -particle source is isotropic over the plane facing the detector, and we cannot directly use the calculated corrections for a monodirectional beam.

ØVERAS²⁸ has treated multiple scattering also for an "isotropic" beam, corresponding to the integration over all incident angles. Example 1) p. 64

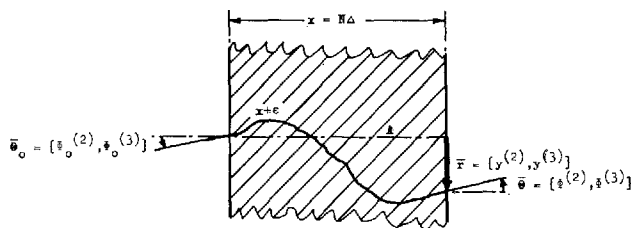


Fig. 7. Exaggerated view of charged particle track suffering multiple scattering in plane layer of material. Symbols are defined in the text.

of ref. 28 fits to our geometry, except that the energy loss of the particles during their passage is neglected. Øveras included the energy loss in several other cases, and it is the aim to present the derivation of the correction for example 1) with energy loss.

The definition of a series of formulas used in Øveras's treatment will be necessary. For further details it is suggested to consult his report.

Formulation of problem: Consider a plane parallel layer of the material with a particle at angular incidence $\bar{\theta}_0 = \{\Phi_0^{(2)}, \Phi_0^{(3)}\}$ as shown in Figure 7. The particle undergoes N small angle scatterings $\bar{\theta}_j$ and emerges at the coordinate $\bar{r} = \{y^{(2)}, y^{(3)}\}$ relative to the line A. $\bar{\theta} = \{\Phi^{(2)}, \Phi^{(3)}\}$ is the angle of emergence.

The pathlength s is then

$$s = x + \varepsilon = \Delta \sum_{j=0}^{N-1} (1 + \bar{\theta}_j^2)^{1/2} \approx N\Delta + \frac{\Delta}{2} \sum_{j=0}^N \bar{\theta}_j^2,$$

where x is the thickness of the layer, ε the correction, and $\Delta = x/N$. The problem is to find ε averaged over all possible paths s .

Probability Distribution: The probability for a single scattering event is approximated by the Gaussian

$$P(\bar{\theta}_j, \bar{\theta}_{j-1}) = \frac{\alpha_j}{\pi \Delta} \exp\left(-\frac{\alpha_j}{\Delta} (\bar{\theta}_j - \bar{\theta}_{j-1})^2\right), \quad (9)$$

where α_j is the mean square space angle per unit length, which gives the best Gaussian fit to MOLIÉRE's theory^{63, 64}.

Distribution of Projected Angle: It is more convenient to express ε in the projected angle $\bar{\chi}_j = \{\xi_j^{(2)}, \xi_j^{(3)}\}$, where $\bar{\chi}_j = \bar{\theta}_j - \bar{\theta}_{j-1}$ for $j \geq 1$, and $\bar{\chi}_0 = \bar{\theta}_0$. Then the mean value $\bar{\varepsilon}$ of ε for all incident angles $\bar{\theta}_0$ can be written

$$\bar{\varepsilon} = \frac{\Delta}{2} \sum_{k, l=0}^N D_{kl} [\overline{\xi_k^{(2)} \xi_l^{(2)}} + \overline{\xi_k^{(3)} \xi_l^{(3)}}] = \bar{\varepsilon}_2 + \bar{\varepsilon}_3, \quad (10)$$

where $D_{kl} = (N - k)$ for $k \geq l, (N - 1)$ for $l \geq k$, and

$$\overline{\xi_k^{(2)} \xi_l^{(2)}} = \overline{\xi_k^{(3)} \xi_l^{(3)}} = \overline{\xi_k \xi_l} = \int_{-\infty}^{\infty} \xi_k \xi_l p(\xi_j | v_\nu) d\xi_0 \dots d\xi_N.$$

$p(\xi_j | v_\nu)$ is the distribution function of the projected angle, in close relation to the probability distribution in eq. (9). p also depends on the experimental geometry—some specific conditions v_ν , usually standing for Φ_0, Φ and y . Average values of quantities projected in the directions (2) and (3) will be the same, because our geometry is symmetric along line A in figure 7.

Energy Loss: α_j in eq. (9) is not constant, but depends on the energy of the decelerated particle. Øveras used the approximate range-energy relation $R = C \cdot E^{1.8}$ to find α_j from α_0 , the mean square spaceangle at the particles entrance into the material.

Fourier Representation: In Øveras's treatment the distribution function $p(\xi_j | v_\nu)$ is transformed to the Fourier representation, and the geometrical conditions take form as Dirac δ -functions

$$\delta\left(\sum_{j=0}^N U_{\nu j} \xi_j - v_\nu\right),$$

where $U_{\nu j}$ is defined in table VI.

The distribution function $p(\xi_j | v_\nu)$ has to be normalized by integration over all ξ_j . The resultant constant $w(v_\nu)$ takes the form

$$w(v_\nu) = \left(\frac{1}{4\pi}\right)^{n/2} \left(\frac{\pi}{a}\right)^{1/2} \frac{1}{\|\sigma_{\nu\nu'}\|^{1/2}} \exp(b^2/4a - c) \quad (11)$$

TABEL VI

v_p	U_{pj}
Φ_0	δ_{j0}
Φ	1
y	$\Delta(N-j)$

where n is the number of conditions v_p defined by the geometry, and

$$\left. \begin{aligned} \sigma_{pp'} &= (\Delta/4) \sum_{j=1}^N U_{pj} U_{p'j} / \alpha_j & a &= 1/4 \sum_{pp'=1}^n U_{p0} U_{p'0} / \sigma_{pp'} \\ b &= 1/2 \sum_{pp'=1}^n U_{p0} v_{p'} / \sigma_{pp'} & c &= 1/4 \sum_{pp'=1}^n v_p v_{p'} / \sigma_{pp'}. \end{aligned} \right\} \quad (12)$$

In this formalism it is possible to give an operative expression for the mean value $\overline{\xi_k \xi_l}$:

$$\overline{\xi_k \xi_l} = \frac{1}{w} \left\{ \frac{\Delta}{2\alpha_k} \delta_{kl} + \frac{\Delta^2}{4\alpha_k \alpha_l} b_k b_l + \left(\frac{\Delta}{2\alpha_k} \delta_{l0} b_k + \frac{\Delta}{2\alpha_l} \delta_{k0} b_l \right) \xi_0 + \xi_0^2 \delta_{k0} \delta_{l0} \right\} w. \quad (13)$$

b_k , b_l , and ξ_0 are operators depending on the geometrical conditions:

$$b_k^\kappa b_l^\lambda \xi_0^\omega = \left(- \sum_{p=1}^n U_{pk} \frac{\partial}{\partial v_p} \right)^\kappa \left(- \sum_{p'=1}^n U_{p'l} \frac{\partial}{\partial v_{p'}} \right)^\lambda \frac{\partial^\omega}{\partial b^\omega}, \quad (14)$$

where κ, λ, ω are arbitrary positive integers.

When inserting (13) into (10), $\bar{\varepsilon}$ can be determined.

Φ_0 and Φ integrated, y specified: This situation corresponds to our special geometry, which is treated in expl 1) of ØVERAS's report²⁸ p. 64 without energy loss. Since only one geometrical condition is present, $n = 1$, and $v_1 = y$. From table VI we get $U_{1k} = \Delta(N - k)$, and we obtain from (11) and (12)

$$\begin{aligned} \sigma_{pp'} &= \sigma_{11} = \frac{\Delta^3}{4} \sum_{k=1}^N (N - k)^2 / \alpha_k, & a &= (N^2 / \Delta) / \sigma_{11}, \\ b &= (\Delta N y / 2) \sigma_{11}, & c &= (y^2 / 4) / \sigma_{11}, \text{ and } w = 1 / (N \Delta). \end{aligned}$$

For the operators defined in eq. (14) we get

$$b_k = -\Delta(N - k) \partial / \partial y, \quad \text{and} \quad b_j = -\Delta(N - j) \partial / \partial y.$$

The operations on w , defined in eq. (11) reduce to

$$\partial w / \partial y = 0, \quad \text{and} \quad \partial w / \partial b = (w \cdot b) / 2a.$$

We are now able to derive $\overline{\xi_k \xi_l}$ in eq. (13) and insert the result in (10) to find $\bar{\varepsilon}$:

$$\bar{\varepsilon}(y) = (\Delta^2/2) \sum_{k=0}^N (N-k)/\alpha_k - (\Delta^2/2N) \sum_{k=0}^N (N-k)^2/\alpha_k + y^2/\Delta N. \quad (15)$$

Energy Loss: The summations in eq. (15) can be expressed as integrals defined by Øveras:

$$A(m) = (6\alpha_0/x^3) \int_0^x (x-\xi)^2/\alpha(\xi) d\xi$$

$$B(m) = (2\alpha_0/x^2) \int_0^x (x-\xi)/\alpha(\xi) d\xi$$

where $m = Qx/R_0$, Q = density of absorber, and R_0 = total range of incident particle. The final result for $y = 0$ is

$$\bar{\varepsilon} = (x^2/12a_0)(3B(m) - A(m)),$$

and table VII shows $\bar{\varepsilon}$ in μgcm^{-2} for some typical energy losses.

TABLE VII

Average increase $\bar{\varepsilon}$ in pathlength of α -particles due to multiple scattering. $\langle T \rangle$ = incident energy, $\langle T_1 \rangle$ = mean exit energy.

$\langle T \rangle = 6.06 \text{ MeV}$		$\langle T \rangle = 8.78 \text{ MeV}$	
$\langle T_1 \rangle / \text{MeV}$	$\bar{\varepsilon} / \mu\text{gcm}^{-2}$	$\langle T_1 \rangle / \text{MeV}$	$\bar{\varepsilon} / \mu\text{gcm}^{-2}$
1	4.0	1	8.0
2	2.4	2	5.8
3	1.3	3	4.0
4	0.5	4	2.4
5	0.1	5	1.6
		6	0.8
		7	0.3

This work supported by Public Health Service Research Grant No. CA-08150 from the National Cancer Institute, and in part by the U.S. Atomic Energy Commission Contract No. AT(04-3)-136.

C. G. Hanke
Danish Engineering Academy
Physics Laboratory B and K
Copenhagen

H. Bichsel
University of Washington
Department of Radiology
Seattle, Washington

References

1. H. BETHE, *Annalen d. Physik* **5**, 325 (1930).
2. M. S. LIVINGSTON and H. A. BETHE, *Rev. Mod. Phys.* **9**, 245 (1937).
3. U. FANO, *Ann. Rev. Nucl. Sci.* **13**, 1 (1963).
4. G. I. HARPER and E. SALAMAN, *Proc. Roy. Soc. A* **127**, 175 (1930).
5. P. JESSE and J. SADAUSKI, *Phys. Rev.* **78**, 1 (1950).
6. J. PHELPS, W. F. HUEBNER, and F. HUTCHINSON, *Phys. Rev.* **95**, 441 (1954).
7. G. ANIANSSON, *Trans. Roy. Inst. Techn. Stockholm, Sweden*, no. 178 (1961).
8. J. BLANDIN - VIAL, *C.R. Acad. Sci.* **254**, 3842 (1962).
9. S. BARKAN, *Istanbul Univ. Fen. Fakultesi Mecmuasi Seri C*, **28**, 71 (1963).
10. J. R. COMFORT, J. F. DECKER, E. T. LYNK, M. O. SCULLY and A. R. QUINTON, *Phys. Rev.* **150**, 249 (1966).
11. R. B. J. PALMER, *Proc. Phys. Soc.* **87**, 681 (1966).
12. E. ROTONDI and K. W. GEIGER, *Nucl. Inst. Meth.* **40**, 192 (1966).
13. H. BICHSEL, *Bull. Am. Phys. Soc.* **6**, 519 (1961).
14. H. L. CHANG, *Range Energy Measurements in Gases*, Thesis, Phys. Dept., Univ. Southern Calif. (1965).
15. H. H. HECKMAN and P. J. LINDSTROM, *Phys. Rev. Lett.* **22**, 871 (1969).
16. H. H. ANDERSEN, H. SIMONSEN and H. SØRENSEN, *Nucl. Phys. A* **125**, 171 (1969).
17. J. J. KOLATA, T. M. AMOS and H. BICHSEL, *Phys. Rev.* **176**, 484 (1968).
18. H. H. ANDERSEN, A. F. GARFINKEL, C. C. HANKE and H. SØRENSEN, *Mat. Fys. Medd. Dan. Vid. Selsk.* **35**, no. 4 (1966).
19. A. RYTZ, *Helv. Phys. Acta* **34**, 240 (1961).
20. E. A. HYDE, I. PERLMAN and G. T. SEABORG, *The Nuclear Properties of the Heavy Elements Vol. 1*, p. 212 (Prentice-Hall 1964).
21. C. TSCHALÄR, Thesis, Phys. Dept. University of Southern Calif. (1967).
22. J. LINDHARD, V. NIELSEN, M. SCHARFF and P. V. THOMSEN, *Mat. Fys. Medd. Dan. Vid. Selsk.* **33**, No. 10 (1963).
23. P. SIFFERT, G. FORCINAL and A. COCHE, *IEEE Trans. Nuclear Sci. NS-14*, 532 (1967).
24. G. ROUX, *Nucl. Instr. Meth.* **33**, 329 (1965).
25. P. EHRHART, W. RUPP, and R. SIZMANN, *phys. stat. sol.* **28**, K 35 (1968).
26. A. CHETHAM-STRODE, J. R. TARRANT, and R. J. SILVA, *IRE Trans. NS* **8**, 59 (1961).
27. C. TSCHALÄR, *Nucl. Inst. Meth.* **61**, 141 (1968).
28. H. ØVERAS, CERN 60-18 (1960).
29. H. W. LEWIS, *Phys. Rev.* **85**, 20 (1951).
30. H. BICHSEL, C. C. HANKE, and J. BÜCHNER, rep. USC-136-148 (1969), Univ. So. Cal., Los Angeles, unpublished.
31. L. M. BROWN, *Phys. Rev.* **79**, 297 (1950).
32. M. C. WALSKE, *Phys. Rev.* **88**, 1283 (1952).

33. M. C. WALSKE, Phys. Rev. **101**, 940 (1956).
34. G. S. KHANDELWAL and E. MERZBACHER, Phys. Rev. **144**, 349 (1966).
35. W. WHALING, Hdb. Phys. **34**, 214 (1958).
36. H. BICHSEL, UCRL - 17538 (1967), unpublished.
37. C. C. HANKE, to be published.
38. M. BOGAARDT and B. KOUDIJS, Physica **18**, 249 (1952).
39. F. MARTIN and L. C. NORTHCLIFFE, Phys. Rev. **128**, 1166 (1962).
40. H. BICHSEL, Nat. Ac. Sci.-Nat. Res. Counc. Publ. 1133, p. 34 second ed. (1967).
41. G. MANO, Ann. de Physique **1**, 407 (1934).
42. R. NAIDU, Ann. de Physique **1**, 72 (1934).
43. M. Y. COLBY and T. N. HATFIELD, Rev. Sci. Instr. **12**, 62 (1941).
44. K. SCHMIEDER, Ann. der Physik **35**, 445 (1939).
45. G. G. EICHHOLZ and N. J. HARRICK, Phys. Rev. **76**, 589 (1949).
46. G. BERTOLINI and M. BETTONI, Nuovo Cim. **1**, 644 (1955).
47. J. J. RAMIREZ, R. M. PRIOR, J. B. SWINT, A. R. QUINTON and R. A. BLUE, Phys. Rev. **179**, 310 (1969).
48. R. L. WOLKE, W. N. BISHOP, E. EICHLER, N. R. JOHNSON and G. D. O'KELLEY, Phys. Rev. **129**, 2591 (1963).
49. H. K. REYNOLDS, D. N. F. DUNBAR, W. A. WENZEL, and W. WHALING, Phys. Rev. **92**, 742 (1953).
50. A. B. CHILTON, J. N. COOPER, and J. C. HARRIS, Phys. Rev. **93**, 413 (1954).
51. J. E. BROLLEY, JR., and F. L. RIBE, Phys. Rev. **98**, 1112 (1955).
52. D. GREEN, J. COOPER, and J. HARRIS, Phys. Rev. **98**, 466 (1955).
53. J. F. JANNI, rep. AFWL-TR-65-150 (1966), Air Force Weapons Laboratory, New Mexico.
54. P. DALTON and J. E. TURNER, Health Physics **15**, 257 (1968).
55. R. J. BELL and A. DALGARNO, Proc. Phys. Soc. **86**, 375 (1965) and **89**, 55 (1966).
56. A. DALGARNO, Proc. Roy. Soc. **76**, 422 (1960).
57. E. BONDERUP, Mat. Fys. Medd. Dan. Vid. Selsk. **35**, no. 17 (1967).
58. J. LINDHARD and M. SCHARFF, Mat. Fys. Medd. Dan. Vid. Selsk. **27**, no. 15 (1953).
59. J. B. MARION and B. A. ZIMMERMAN, Nucl. Instr. Meth. **51**, 93 (1967).
60. C. N. YANG, Phys. Rev. **84**, 599 (1951).
61. H. BICHSEL and E. A. UEHLING, Phys. Rev. **119**, 1670 (1960).
62. C. TSCHALÄR and H. BICHSEL, Nucl. Inst. Meth. **62**, 208 (1968).
63. G. MOLIERE, Z. Naturforsch. **2a**, 133 (1947).
64. G. MOLIERE, Z. Naturforsch. **3a**, 78 (1948).
65. H. BICHSEL, Phys. Rev. **B1**, 2854 (1970).
66. J. B. SWINT, R. M. PRIOR and J. J. RAMIREZ, Nucl. Inst. Meth. **80**, 134 (1970).



